Japan Bilingual Publishing Co.

New Environmentally-Friendly Materials
https://ojs.bilpub.com/index.php/nefm

ARTICLE

Morphology and Functional Behavior of Polyacrylamide Hydrogels Reinforced with Sustainable Montmorillonite Nanoclay

Abayomi I. Adeleke [1] ***, Jonathan R. Sanders*** [1*] ***, Pedro E. Arce*** [1,2*]

[1] *Biomolecular Medicine Laboratory, Chemical Engineering, Tennessee Technological University, Cookeville, TN 38505, USA*

[2] *Environmental Catalysis Laboratory, Chemical Engineering, Tennessee Technological University, Cookeville, TN 38505, USA*

ABSTRACT

Polyacrylamide (PAAM) hydrogels are widely used in electrophoretic separations of proteins, deoxyribonucleic acid (DNA), and cells due to their high resolving power, optical and ultraviolet (UV) transparency, electro-neutrality, and tunable pore structure. Incorporation of nanomaterials into PAAM gels has been proposed as a strategy to further tailor gel microstructure and transport properties. In this study, sodium montmorillonite (Na-MMT) nanoplatelets, a naturally occurring nanoclay with an average diameter of ~400 nm and an aspect ratio of ~150, were incorporated into PAAM gels to form nanocomposite hydrogels, and their effects on protein mobility were systematically investigated. Native polyacrylamide gel electrophoresis revealed that Na-MMT incorporation consistently reduced protein mobility relative to pure PAAM gels. To elucidate the origin of this behavior, rheological measurements and scanning electron microscopy (SEM) were employed. Rheological analysis showed that pure PAAM gels exhibited greater elasticity than nanocomposite gels, attributed to disruption of the polymer network by nanoplatelet incorporation and extended sonication during sample preparation. SEM image analysis further revealed the absence of well-defined matrix cells in the nanocomposite gels. Instead, osmotic-pressure-driven nanoparticle aggregation produced

*CORRESPONDING AUTHOR:
Jonathan R. Sanders, Biomolecular Medicine Laboratory, Chemical Engineering, Tennessee Technological University, Cookeville, TN 38505, USA; Email: rsanders@tntech.edu; Pedro E. Arce, Biomolecular Medicine Laboratory, Chemical Engineering, Tennessee Technological University, Cookeville, TN 38505, USA; Environmental Catalysis Laboratory, Chemical Engineering, Tennessee Technological University, Cookeville, TN 38505, USA; Email: parce@tntech.edu

ARTICLE INFO
Received: 12 July 2025 | Revised: 8 October 2025 | Accepted: 16 October 2025 | Published Online: 23 October 2025
DOI: https://doi.org/10.55121/nefm.v4i2.747

CITATION
Adeleke, A.I., Sanders, J.R., Arce, P.E., 2025. Morphology and Functional Behavior of Polyacrylamide Hydrogels Reinforced with Sustainable Montmorillonite Nanoclay. New Environmentally-Friendly Materials. 4(2): 43–54. DOI: https://doi.org/10.55121/nefm.v4i2.747

dense, poorly interconnected nanopores that impeded effective protein transport. These structural changes led to reduced electrophoretic mobility and separation efficiency. Overall, the findings demonstrate that PAAM–bentonite nanocomposite hydrogels exhibit inherent microstructural limitations for electrophoretic applications, emphasizing the need for precise control of nanoparticle dispersion and gel architecture in the design of nanocomposite separation media.
Keywords: Polyacrylamide (PAAM); Nanocomposite; Bentonite; Sodium Montmorillonite (Na-MMT); Nanoclay; Electrophoresis; Hydrogel

1. Introduction

The manufacturability of polymer nanocomposites is critical for advancing soft, smart, and high-performance materials. To achieve next-generation materials with enhanced properties, the incorporation of nanofillers—among other technologies—has attracted significant attention from researchers [1–4]. Introducing nanofillers into the polymer matrix creates a pathway to harness the unique properties of nanoparticles, such as improved mechanical strength, stability, and thermal conductivity [4,5]. When these advantages are combined with the flexibility, transparency, and lightness of polymer materials [6–8], nanocomposites with advanced capabilities can be manufactured.

Polyacrylamide (PAAM) has been extensively studied for various applications such as polyacrylamide gel electrophoresis (PAGE) [2,9–12], biomedical applications [13–16], and for several environmental applications such as waste disposal [17], oil field applications [18], and several others. During polymerization, PAAM forms a porous network that creates versatile gels. These gels are produced by polymerizing acrylamide with a cross-linker, initiated by ammonium persulfate (APS) and catalyzed by N,N,N',N'-tetramethylethylenediamine (TEMED). PAAM is valued for its resolving power, adaptability, stability, simplicity, and cost-effectiveness in electrophoresis applications [8,19]. It is rapidly becoming the standard medium for electrophoresis in clinical applications [15,20,21].

Several attempts have been made to improve the performance of polyacrylamide gels. Some of these attempts include the introduction of nanoparticles [4,16,22–24], or other pretreatments such as electrostatic potential pre-electrophoresis [19] and magnetic field pre-electrophoresis [23–25]. The use of Sodium Montmorillonite (Na-MMT) as nano fillers in PAAM gels and the effects on the gel structure on the macroscopic scale have also been reported [26–28]. However, the microscopic interactions and structural changes are yet to be fully characterized.

This article explores the manufacturability and separation efficiency of polyacrylamide—sodium montmorillonite (PAAM Na-MMT) nanocomposite gel using both sodium dodecyl sulphate (SDS) and native electrophoresis methods. Our approach employs Na-MMT, a naturally abundant and environmentally benign nanoclay, to fabricate nanocomposite hydrogels with unusually low polymer content. By leveraging this sustainable filler strategy, we examine how nanoscale interactions between exfoliated nanoplatelets and polymer chains influence the macroscopic properties of the gel. First, Na-MMT nanoplatelets were characterized, and both sodium dodecyl sulphate–polyacrylamide gel electrophoresis (SDS-PAGE) and Native Polyacrylamide Gel Electrophoresis (Native-PAGE) were used to probe the effect of the nanofillers on PAGE. Finally, attention was turned to characterizing the structure of polyacrylamide gel manufactured and identifying the nanoscale interactions responsible for the macroscale properties of the polyacrylamide nanocomposite. This study uniquely bridges the gap between microstructural morphology and bulk electrophoretic behavior, offering a clearer understanding of the design–performance relationship in green nanocomposite gels.

2. Materials and Methods

The concentrations of reagents in the hydrogels are described using two terms: %T, the total monomer concentration (w/v), and %C (the percentage of crosslinker (bis-acrylamide) relative to the total monomer mass) [19]. Adjusting %T and %C controls the gel's pore size and density, which in turn affects separation capabilities. In this contribution, 6% T and 3.3% C gels were studied and analyzed. This approach allows the use of a considerably lower amount of PAAM. Using a lower PAAM concentration is environmentally significant because it reduces toxic monomer usage, minimizes synthetic polymer waste, and lowers the overall chemical

and energy footprint of hydrogel fabrication [1]. **Table 1** summarizes all reagents used for gel fabrication, including protogel, running and resolving buffers, stacking buffers, protein solvent, protein samples, and Na-MMT nanoparticles.

Table 1. Reagents for gel fabrication.

Reagents	Source	Compound	Properties
Protogel	Themo Fisher	Polyacrylamide/Bis-acrylamide	pH 6.5
Running buffer	BIO-RAD	Tris/Glycine/(SDS)	pH 8.3
Resolving buffer	Thermo Fisher	Tris	pH 8.8
Stacking buffer	Thermo Fisher	Tris-HCl	pH 6.8
Protein solvent	Fisher Scientific	PBS	pH 7.3
Protein	MP, Themo Fisher, BIO-RAD	Carbonic Anhydrase (CA), Ovalbumin (OSA), Kaleidoscope Ladder	–
Nanoparticle	MP Biomedicals	Bentonite/Na-MMT	pH 10

Na-MMT was prepared by dispersing and exfoliating 1 g of Na-MMT in 100 mL of water. The suspension underwent 90 minutes of sonication, followed by 24 h of continuous stirring, and an additional 30 min sonication step. It was then centrifuged at 1000 rpm (180 g) for one hour to remove coarse aggregates and residual impurities. The resulting stock suspension was characterized by dynamic light scattering and SEM to verify nanoplatelet dispersion quality. A more detailed explanation of the procedure has been described previously in the literature [25,29].

To prepare PAAM–Na-MMT nanocomposite gels, reagents were formulated to yield a 6% T solution containing varying Na-MMT concentrations (0.021%, 0.109%, and 0.216%) following the protocol described by Haris et al. [19]. Control samples without nanoplatelets were prepared using the same procedure. The gel casting setup involved two glass plates, one plate notched to accommodate the gel comb, and spacers placed along the edges. The plates and spacers were positioned in a casting box and secured within a casting frame to prevent leakage. The gel thickness was maintained at a standard 0.7 mm in this study.

2.1. Dynamic Light Scattering (DLS)

For particle size by DLS, the nanoplatelet suspension was first diluted to 10^{-4}–10^{-5} g/L. DLS measurements were then performed in Malvern Zetasizer nano series to monitor the particle size in the 0.3–10,000 nm range. Before DLS analysis, the nanoplatelets were exfoliated using the process described above.

2.2. Native-PAGE

Native-PAGE separates proteins while preserving their native conformation, charge, and intermolecular interactions. Ovalbumin (OSA) and carbonic anhydrase (CA) were dissolved in 10 × phosphate buffer saline (PBS, pH 7.3) at 1 mg/mL. A 4 × Laemmli sample buffer dye (Bio-Rad), diluted 1:4 with the protein solution, was used for staining. For analysis, 10 µL of each protein sample—either pure OSA, pure CA, or a premixed 1:1 combination, was loaded into designated gel wells. Electrophoresis was performed at 100 V for 90 min.

2.3. SDS-PAGE

SDS-PAGE was performed using Precision Plus Protein™ Kaleidoscope™ prestained protein standard. For the electrophoresis, 10 µL aliquots of protein samples were carefully pipetted into the designated gel lanes. Electrophoresis was conducted at 100 V for 90 min; current was not controlled.

2.4. Rheology Studies

Rheological experiments were conducted using a stress-controlled rotational rheometer (TA Instruments, AR 550) equipped with a Peltier temperature-control system.

The setup featured two parallel stainless-steel plates (20 mm diameter) with the sample positioned between them. The upper plate of the AR550 rotated to apply strain, while the lower plate remained stationary, transmitting torque to the Normal Force Transducer (NFT). The data were processed by integrated software, which converted them into rheological parameters. Strain (γ) was calculated using $\gamma \approx \theta R/h$, with $\theta(t)$ being the angular displacement, R the plate radius, and h the distance between plates, set to 1000 μm. All experiments were conducted at 25 °C with a minimum sample volume of 0.314 mL. Daily calibrations and mappings were performed before experiments.

2.5. SEM Imaging

Scanning Electron Microscopes (SEM) require fully dehydrated samples due to their vacuum environment, necessitating thorough drying of samples that naturally contain liquids. For this study, hydrogels were fixed, washed, and serially dehydrated with progressively increasing concentrations of ethanol solutions before using the critical point dryer (CPD) to dry the gel samples. Because conductivity is crucial for SEM imaging, organic samples were mounted on carbon tape and coated with a thin layer of conductive metal. Specifically, Au-Pt coating was applied, and imaging was performed using an ultra-high-resolution Field Emission SEM (FE-SEM), Hitachi SU7000, at Tennessee Technological University. The SU7000 was equipped with an enhanced energy dispersive spectroscopy (EDS) system (Octane Elect) and APEX™ software by EDAX, which were used to examine the elemental composition of the MMT nanoplatelets.

3. Results

3.1. Nanoplatelet Exfoliation

Bentonite (Na-MMT) was exfoliated into nanoplatelets and characterized using dynamic light scattering (DLS). DLS results showed a monomodal particle-size distribution with a peak near 400 nm (**Figure 1**), indicating effective nanoclay exfoliation. This value aligns with previously reported Na-MMT dimensions [29,30].

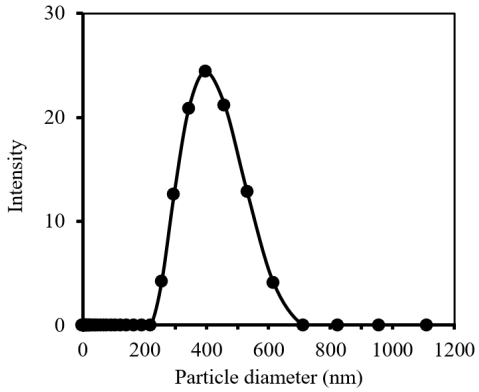

Figure 1. Particle-size distribution of Na-MMT.

To further verify platelet morphology, the measured particle diameter (~400 nm) from DLS experiments and the applied centrifugal acceleration (~180 g) were used to estimate the aspect ratio of exfoliated Na-MMT. This calculation was based on an empirical correlation developed by Ploehn and Liu [29], which relates sedimentation behavior to nanoplatelet geometry. The resulting aspect ratio was approximately 150, indicating that the exfoliated structures predominantly exist as individual nanoplatelets rather than multilayer tactoids. This high aspect ratio aligns with expected morphological characteristics of well-dispersed clay nanofillers and is essential for achieving uniform distribution and strong interfacial interactions within polymer matrices. Together, the DLS results and the correlation-based analysis confirm that the exfoliation strategy employed here successfully yielded high-aspect ratio Na-MMT nanoplatelets suitable for incorporation into the PAAM gel matrix.

3.2. Gel Electrophoresis

To evaluate the influence of Na-MMT nanoplatelets on protein mobility, SDS-PAGE and Native-PAGE

were performed at a constant 100 V. Protein migration distances were measured for the smallest ladder protein in SDS-PAGE, while in Native-PAGE, the distance was measured from the top of the resolving gel to the center of the OSA/CA band, reflecting their similar molecular masses. The control sample consisted of pure PAAM gels, and nanocomposite gels were prepared with Na-MMT volume fractions (Ø) of 0.021%, 0.109%, and 0.216%. All migration distances were normalized to the mobility (u) of the control sample and measured using ImageJ software [3]. The resulting trends are presented in **Figure 2**.

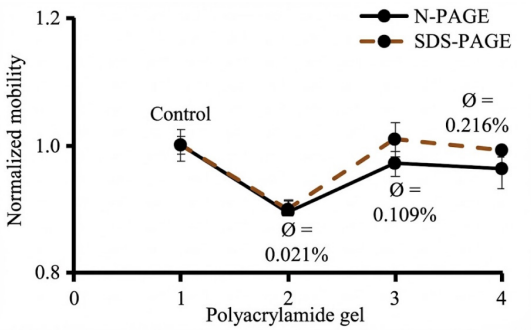

Figure 2. Effects of increasing Na-MMT volume fraction on 6% T PAGE.

To interpret the observed behavior, the migration trends in Native-PAGE were compared with those from SDS-PAGE, and both showed a similar reduction in mobility when using the smallest volume fraction of 0.021%, but these values returned to control levels at higher volume fractions. While protein mobility in PAGE is typically governed by molecular size, shape, and charge-to-mass ratio [19,31–33], the consistent trend across both electrophoresis modes suggests an additional influence from the nanoplatelets. Prior studies have reported that nanoparticles can either enhance or reduce protein mobility depending on their interactions with the polymer matrix. For example, Sajjadi et al. [16] observed improved separation in SDS-PAGE with surface-modified SiO_2 nanoparticles, whereas other researchers have reported the opposite effect [22,34]. For example, Huang et al. [22] reported reduced mobility in TiO_2–PAAM gels due to altered thermal dissipation. Our results align with this latter behavior, indicating that nanoplatelets introduce nanoscale interactions that affect the macroscopic transport of proteins [33].

3.3. Rheological Studies

3.3.1. Linearity Test

Strain-sweep measurements (**Figure 3**) showed that storage modulus (G') was independent of strain amplitude for all samples, confirming linear viscoelastic behavior within the tested range. Based on these results, a strain of 10% was selected for subsequent frequency and time-sweep experiments. Across all samples, G' remained independent of strain amplitude and exceeded viscous modulus (G''), confirming gel-like behavior and supporting the use of 10% strain for subsequent tests.

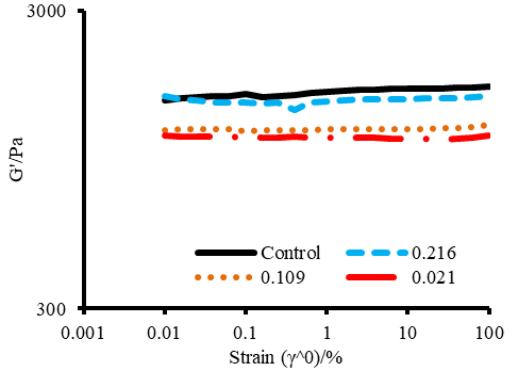

Figure 3. Strain Sweep to determine the onset of nonlinearity in dynamic testing.

3.3.2. Frequency Sweeps and Loss Factor

Frequency sweeps (**Figure 4**) showed that pure PAAM gels exhibited the highest storage modulus, while all nanocomposite samples displayed reduced G' values. This decrease reflects disruption of elastic junctions within the polymer network by the nanoplatelets and may also be influenced by the extended sonication required for nanoparticle dispersion [35,36]. The 0.021% and 0.109% MMT samples exhibited similar G' values despite differing nanoplatelet loadings, suggesting that agglomeration limits the effective contribution of the platelets to network elasticity. The 0.216% MMT sample showed the lowest value of G', consistent with poorer dispersion and more extensive aggregation at higher nanoplatelet concentrations [18,36,37].

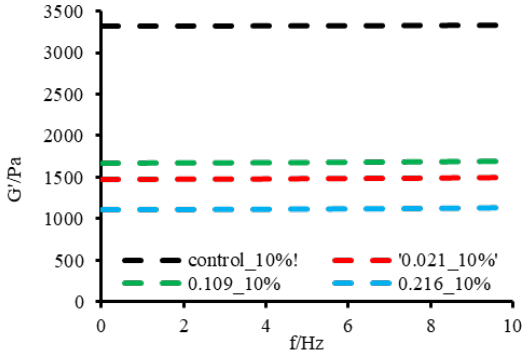

Figure 4. Frequency sweeps as a function of f(Hz) for all materials.

Loss factor trends (**Figure 5**) showed that G' remained much greater than G", confirming predominantly elastic behavior for all samples. At higher nanoplatelet loadings (0.109% and 0.216%), tan δ increased modestly, indicating greater viscous dissipation, consistent with prior observations that nanoparticle-filled gels exhibit enhanced viscous contributions at higher filler concentrations [30]. This behavior also suggests stronger interfacial interactions between nanoplatelets and polymer chains, which are known to arise from nanoparticle agglomeration and the cumulative effect of particle–polymer contacts [38–40].

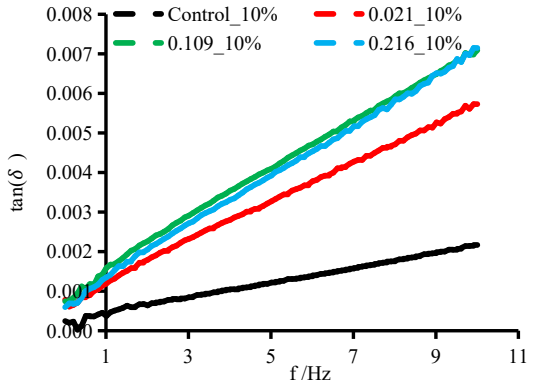

Figure 5. Frequency sweep: Loss factor as a function of f(Hz).

3.3.3. Time Sweep Tests: Cast to Cure

Time-sweep measurements (**Figure 6**) were used to monitor the evolution of G' during gelation. The pure PAAM samples exhibited the highest modulus, while all nanocomposite samples showed reduced G', consistent with earlier evidence of nanoplatelet-induced disruption of elastic junctions. Notably, the 0.021% and 0.109% MMT samples displayed nearly identical G' throughout gelation, suggesting that nanoplatelet agglomeration limits their effective contribution to the network, in agreement wiAth reported aggregation-driven reductions in junction density [18,37,41]. The

0.216% MMT sample showed the lowest G' and the largest strain-dependent differences, further indicating that extensive aggregation at higher nanoplatelet loading restricts the formation of elastically effective junctions.

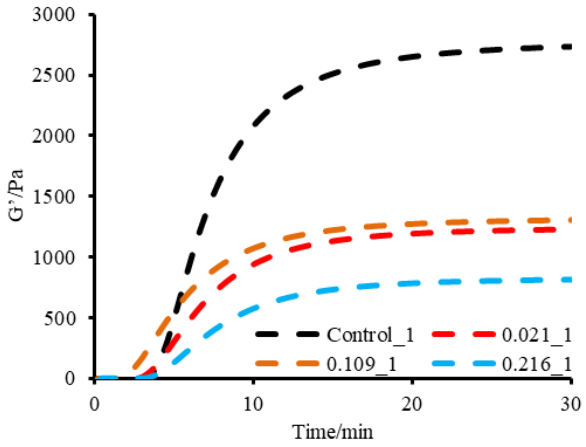

Figure 6. Storage modulus of all samples at γ = 10%.

3.4. SEM Imaging

Figure 7 shows the polymer matrix of the pure PAAM gel, revealing the characteristic 'cell' structures previously described by Thompson et al. [25]. Two primary elements can be observed: the larger 'cells,' which form the dominant framework of the gel, and the smaller pores embedded within them. The cells and nanopores are envisioned as the main pathways for macromolecular transport, playing a central role in determining electrophoretic mobility. This structural interpretation is consistent with reptation-based models of migration, in which proteins move through a sequence of pores of varying sizes as they traverse the gel network [42–45].

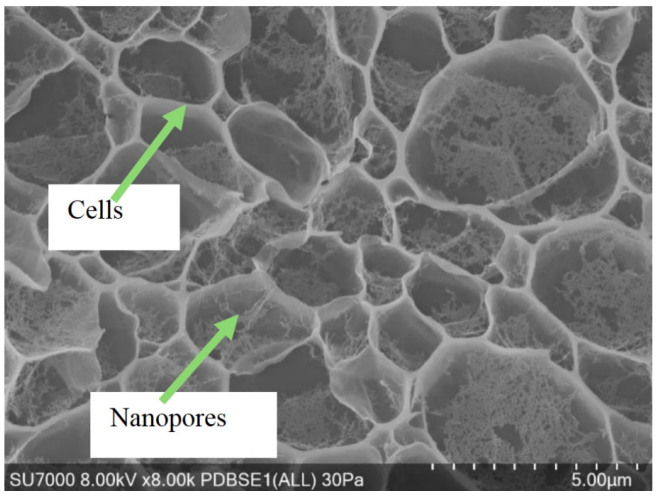

Figure 7. Image of control sample matrix.

The second major structural element visible in the pure PAAM gels is the network of nanopores located within the larger cell structures. These smaller features serve as additional barriers to protein migration, offering more refined pathways through the gel matrix. Given the relative size of protein molecules, it is reasonable to consider the cells as the primary migration channels, while the nanopores contribute to separation by imposing secondary size-dependent resistance. Within the framework of the reptation model, proteins navigate through a sequence of cells and interact with the nanopores, which helps to explain the molecular separation effects observed during

electrophoresis [45,46].

Figure 8a,b shows the polymer matrix in PAAM–bentonite nanocomposites. In contrast to the pure gels, the nanocomposite samples contain very few recognizable cells and are instead dominated by nanopores. This structural shift aligns with rheological results, which showed reduced G' in all nanocomposite formulations (**Figures 4** and **6**). The loss of larger cell structures also aligns with the electrophoresis performance in SDS-PAGE. Six clearly resolved protein bands were observed in the pure gels (data not shown), whereas only five bands appeared in the nanocomposite gels, indicating diminished separation capability, which is posited to be associated with physical effects of the bentonite on both the cell and nanopore domains.

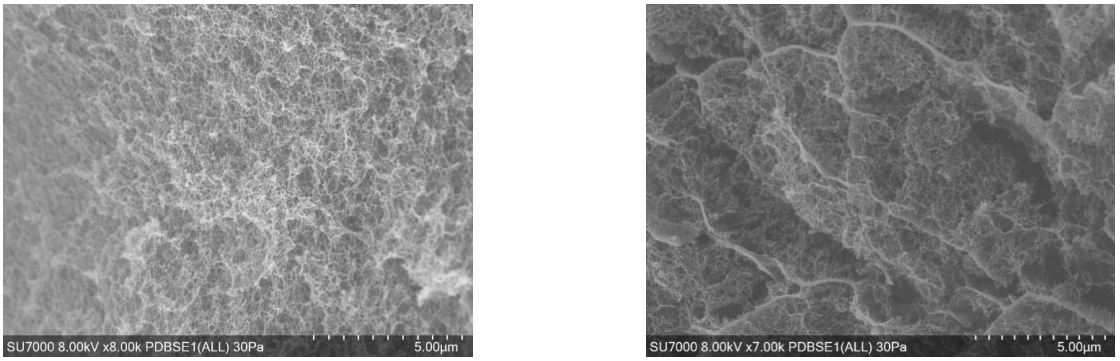

(**a**) (**b**)

Figure 8. SEM Image of polymer matrix sample: (**a**) 0.109% MMT; (**b**) 0.216% MMT.

Overall, rheology tests and SEM images confirm that incorporating Na-MMT nanoplatelets alters gel architecture by reducing the prevalence of cell structures and promoting a nanopore-dominated matrix. This structural modification, likely influenced by nanoplatelet interactions and extended sonication required for dispersion, explains the lower storage modulus and reduced separation efficiency observed in nanocomposite gels.

Although exfoliation and extended sonication were intended to promote uniform Na-MMT dispersion, rheological results suggest significant nanoplatelet aggregation within nanocomposite gels. In **Figure 9**, the SEM image confirms this behavior, showing clusters of platelets rather than a fully dispersed network. This aggregation aligns with the reduced number of cell structures observed in nanocomposite matrices and reflects the inherent tendency of high-aspect-ratio nanoplatelets to aggregate within the polymer network. These structural features explain the reduced mechanical stiffness and altered transport behavior of PAAM–MMT gels observed earlier.

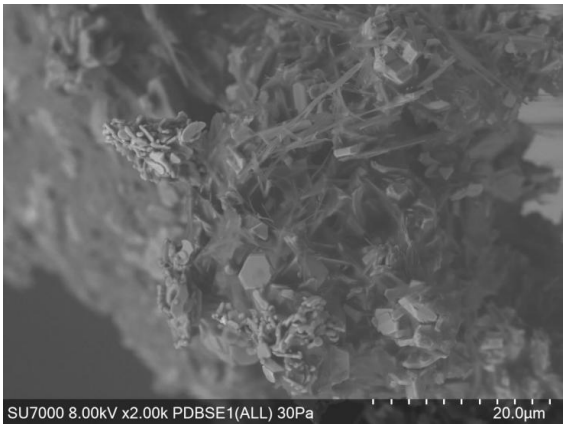

Figure 9. SEM Image of MMT nanoplatelets in 0.216% sample.

The aggregation shown in the SEM image of the 0.216% MMT sample (**Figure 9**) aligns with the depletion mechanism described by Asakura and Oosawa [47], whereby high–aspect-ratio platelets experience attractive forces

in polymer-rich environments, promoting cluster formation. In the nanocomposite gels, such interactions lead to platelet aggregates that are sometimes located outside the polymer-rich domains, reducing the formation of continuous load-bearing junctions. The aggregate size also increases with nanoplatelet concentration, in agreement with prior reports on filler-induced clustering in polymer nanocomposites [48–50]. These observations provide additional evidence that nanoplatelet agglomeration during gel curing plays a central role in the reduced mechanical stiffness and altered microstructure of the PAAM–MMT gels. While it does not appear that the presence of the bentonite significantly affects the overall separation-enabling features of the PAAM gels at the higher concentrations of bentonite, there clearly is an effect on the mechanical properties of such gels.

4. Conclusions

This study demonstrates the successful exfoliation of sodium montmorillonite (Na-MMT), a naturally abundant and environmentally benign nanoclay, and its incorporation into polyacrylamide (PAAM) hydrogels. The resulting nanoplatelets (~400 nm, aspect ratio ~150) enabled low-polymer-content gel fabrication but introduced notable microstructural and mechanical changes. In both SDS-PAGE and Native-PAGE, protein (CA and OSA) mobility was reduced in PAAM–MMT nanocomposites relative to pure PAAM gels at the lowest concentration of bentonite tested. Rheological and SEM analyses revealed that this decline stems from nanoplatelet agglomeration during gelation, which disrupts elastic junctions and replaces the robust, cell-based architecture of pure PAAM with nanopore-dominated networks.

While Na-MMT offers clear sustainability advantages as a low-cost, natural nanofiller, its aggregation behavior may limit its effectiveness in electrophoretic applications. These findings highlight both the promise and challenges of clay-based nanocomposites in environmentally conscious materials design. Future work should explore dispersion control and surface modification strategies to fully realize the potential of Na-MMT-enhanced hydrogels for green, high-performance separation technologies.

Author Contributions

Conceptualization, P.E.A. and J.R.S.; methodology, A.I.A., and J.R.S.; software, A.I.A., and J.R.S.; validation, A.I.A., J.R.S. and P.E.A.; formal analysis, A.I.A.; investigation, A.I.A.; resources, P.E.A., and J.R.S.; data curation, A.I.A.; writing—original draft preparation, A.I.A.; writing—review and editing, A.I.A., J.R.S. and P.E.A.; visualization, A.I.A.; supervision, J.R.S. and P.E.A.; project administration, J.R.S. and P.E.A.; funding acquisition, J.R.S. and P.E.A. All authors have read and agreed to the published version of the manuscript.

Funding

This work was supported by the Center for Manufacturing Research (CMR) at Tennessee Technological University and the Chemical Engineering Department at Tennessee Technological University.

Institutional Review Board Statement

Not applicable.

Informed Consent Statement

Not applicable.

Data Availability Statement

The data supporting the findings of this study are available from the corresponding author upon reasonable request. Datasets were stored locally and not publicly available.

Acknowledgments

The authors wish to acknowledge and thank the Center for Manufacturing Research (CMR) at Tennessee Tech University for providing access and financial support for using the SEM facility. Also, authors thank Micah Midgett for providing the necessary training to operate the equipment.

Conflicts of Interest

The authors declare no conflict of interest.

References

[1] Dejene, B.K., 2024. Advancing Natural Fiber-Reinforced Composites Through Incorporating ZnO Nanofillers in the Polymeric Matrix: A Review. Journal of Natural Fibers. 21(1), 2356015. DOI: https://doi.org/10.1080/15440478.2024.2356015

[2] Hajba, L., Jeong, S., Chung, D.S., et al., 2023. Capillary Gel Electrophoresis of Proteins: Historical Overview and Recent Advances. TrAC Trends in Analytical Chemistry. 162, 117024. DOI: https://doi.org/10.1016/j.trac.2023.117024

[3] Khan, I., Khan, I., Saeed, K., et al., 2023. Polymer Nanocomposites: An Overview. In: Ali, N., Bilal, M., Khan, A., et al. (Eds.). Smart Polymer Nanocomposites: Design, Synthesis, Functionalization, Properties, and Applications. pp. 167–184. DOI: https://doi.org/10.1016/B978-0-323-91611-0.00017-7

[4] Chandran, A.J., Rangappa, S.M., Suyambulingam, I., et al., 2024. Micro/Nano Fillers for Value-Added Polymer Composites: A Comprehensive Review. Journal of Vinyl and Additive Technology. 30(5), 1083–1123. DOI: https://doi.org/10.1002/vnl.22106

[5] Guo, D., Xie, G., Luo, J., 2014. Mechanical Properties of Nanoparticles: Basics and Applications. Journal of Physics D: Applied Physics. 47(1), 013001. DOI: https://doi.org/10.1088/0022-3727/47/1/013001

[6] Mouchati, A., Yagoubi, N., 2023. Mechanical Performance and Cytotoxicity of an Alginate/Polyacrylamide Bipolymer Network Developed for Medical Applications. Materials. 16(5), 1789. DOI: https://doi.org/10.3390/ma16051789

[7] Razmjooee, K., Ahmady, A.R., Arabzadeh, N., et al., 2023. Synthesis of Gelatin/Polyacrylamide/Carboxymethyl Chitosan Triple-Network Hydrogels and Evaluation of Their Properties for Potential Biomedical Applications. Materials Science and Engineering: B. 295, 116597. DOI: https://doi.org/10.1016/j.mseb.2023.116597

[8] Awasthi, S., Gaur, J.K., Bobji, M.S., et al., 2022. Nanoparticle-Reinforced Polyacrylamide Hydrogel Composites for Clinical Applications: A Review. Journal of Materials Science. 57(17), 8041–8063. DOI: https://doi.org/10.1007/s10853-022-07146-3

[9] Packirisamy, V., Pandurangan, P., 2023. Polyacrylamide Gel Electrophoresis: A Versatile Tool for the Separation of Nanoclusters. BioTechniques. 74(1), 51–62. DOI: https://doi.org/10.2144/btn-2022-0086

[10] Sule, R., Rivera, G., Gomes, A.V., 2022. Western Blotting (Immunoblotting): History, Theory, Uses, Protocol and Problems. BioTechniques. 75(3), 99–114. Available from: https://www.tandfonline.com/doi/full/10.2144/btn-2022-0034

[11] Arakawa, T., Nakagawa, M., Tomioka, Y., et al., 2022. Gel-Electrophoresis Based Method for Biomolecular Interaction. Methods in Cell Biology. 169, 67–95. DOI: https://doi.org/10.1016/bs.mcb.2021.12.030

[12] Takemori, A., Kaulich, P.T., Cassidy, L., et al., 2022. Size-Based Proteome Fractionation through Polyacrylamide Gel Electrophoresis Combined With LC–FAIMS–MS for In-Depth Top-Down Proteomics. Analytical Chemistry. 94(37), 12815–12821. Available from: https://pubs.acs.org/doi/abs/10.1021/acs.analchem.2c02777

[13] Wang, J., Xu, Y., Li, S. et al., 2025. Physical Entanglement Improves the Anti-adsorption and Super-Lubricity Properties of Polyacrylamide-Based Hydrogels for Biomedical Applications. Advanced Composites and Hybrid Materials. 8(2), 208. DOI: https://doi.org/10.1007/s42114-025-01267-4

[14] Gelfi, C., Righetti, P.G., 1981. Polymerization Kinetics of Polyacrylamide Gels I. Effect of Different Cross-Linkers. Electrophoresis. 2(4), 213–219. DOI: https://doi.org/10.1002/elps.1150020404

[15] Li, C., Arakawa, T., 2019. Application of Native Polyacrylamide Gel Electrophoresis for Protein Analysis: Bovine Serum Albumin as a Model Protein. International Journal of Biological Macromolecules. 125, 566–571. DOI: https://doi.org/10.1016/j.ijbiomac.2018.12.090

[16] Sajjadi, S.H., Ahmadzadeh, H., Goharshadi, E.K., 2020. Enhanced Electrophoretic Separation of Proteins by Tethered SiO_2 Nanoparticles in an SDS-Polyacrylamide Gel Network. The Analyst. 145(2), 415–423. DOI: https://doi.org/10.1039/C9AN01759C

[17] Sojka, R.E., Bjorneberg, D.L., Entry, J.A., et al., 2007. Polyacrylamide in Agriculture and Environmental Land Management. Advances in Agronomy. 92, 75–162. DOI: https://doi.org/10.1016/S0065-2113(04)92002-0

[18] Li, J., Zhou, W., Qi, Z., et al., 2019. Morphology and Rheological Properties of Polyacrylamide/Bentonite Organic Crosslinking Composite Gel. Energies. 12(19), 3648. DOI: https://doi.org/10.3390/en12193648

[19] Haris, A., Sanders, J.R., Arce, P.E., 2020. Influence of Pre-Electrophoresis on Protein Separations in Poly-

acrylamide Gels. Journal of Applied Polymer Science. 137(34), 48994. DOI: https://doi.org/10.1002/app.48994

[20] Green, M.R., Sambrook, J., 2020. Polyacrylamide Gel Electrophoresis. Cold Spring Harbor Protocols. 2020(12), pdb.prot100412. DOI: https://doi.org/10.1101/pdb.prot100412

[21] Kügler, M., Jänsch, L., Kruft, V., et al., 1997. Analysis of the Chloroplast Protein Complexes by Blue-Native Polyacrylamide Gel Electrophoresis. Photosynthesis Research. 53(1), 35–44.

[22] Huang, G., Zhang, Y., Ouyang, J., et al., 2006. Application of Carbon Nanotube-Matrix Assistant Native Polyacrylamide Gel Electrophoresis to the Separation of Apolipoprotein A-I and Complement C3. Analytica Chimica Acta. 557(1–2), 137–145. DOI: https://doi.org/10.1016/j.aca.2005.10.050

[23] Cai, J., Zhao, H., Liu, H., et al., 2024. Magnetic Field Vertically Aligned Co-MOF-74 Derivatives/Polyacrylamide Hydrogels With Bifunction of Excellent Electromagnetic Wave Absorption and Efficient Thermal Conduction Performances. Composites Part A: Applied Science and Manufacturing. 176, 107832. DOI: https://doi.org/10.1016/j.compositesa.2023.107832

[24] Wang, K., Wen, J., Zhang, S., et al., 2024. Magnetic Polyacrylamide-Based Gel with Tunable Structure and Properties and Its Significance in Conformance Control of Oil Reservoirs. Colloids and Surfaces A: Physicochemical and Engineering Aspects. 702, 135093. DOI: https://doi.org/10.1016/j.colsurfa.2024.135093

[25] Thompson, J.W., Stretz, H.A., Arce, P.E., et al., 2012. Effect of Magnetization on the Gel Structure and Protein Electrophoresis in Polyacrylamide Hydrogel Nanocomposites. Journal of Applied Polymer Science. 126(5), 1600–1612. DOI: https://doi.org/10.1002/app.36660

[26] Lima, B.L.B., Araújo, M.J.F., Souza, E.A., et al., 2025. Hydrogels Based on Polyacrylamide and Bentonite for Trapped Annular Pressure Mitigation. Journal of Molecular Liquids. 434, 127989. DOI: https://doi.org/10.1016/j.molliq.2025.127989

[27] Oppong, S.A., Mandal, M., Ojha, K., 2023. Synthesis and Optimization of Bentonite Enforced Poly(Acrylamide/Co-Sodium Dodecylbenzensulfonate) Preformed Particle Gels for Conformance Control in High Salinity Reservoirs. Petroleum Science and Technology. 41(5), 546–563. DOI: https://doi.org/10.1080/10916466.2022.2063333

[28] Siryk, O., Goncharuk, O., Samchenko, Y., et al., 2024. Comparison of Structural, Water-Retaining and Sorption Properties of Acrylamide-Based Hydrogels Cross-Linked by Physical and Chemical Methods. ChemPhysChem. 25(4), e202300812. Available from: https://chemistry-europe.onlinelibrary.wiley.com/doi/abs/10.1002/cphc.202300812

[29] Ploehn, H.J., Liu, C., 2006. Quantitative Analysis of Montmorillonite Platelet Size by Atomic Force Microscopy. Industrial & Engineering Chemistry Research. 45(21), 7025–7034. DOI: https://doi.org/10.1021/ie051392r

[30] Noskov, A.V., Alekseeva, O.V., Shibaeva, V.D., et al., 2020. Synthesis, Structure and Thermal Properties of Montmorillonite/Ionic Liquid Ionogels. RSC Advances. 10(57), 34885–34894. DOI: https://doi.org/10.1039/D0RA06443B

[31] Bhatt, M., Rai, V., Kumar, A., et al., 2022. SDS-PAGE and Western Blotting: Basic Principles and Protocol. In: Deb, R., Yadav, A.K., Rajkhowa, S., et al. (Eds.). Protocols for the Diagnosis of Pig Viral Diseases. Springer: New York, NY, USA. pp. 313–328. DOI: https://doi.org/10.1007/978-1-0716-2043-4_23

[32] Sugiyama, Y., Uezato, Y., 2022. Analysis of Protein Kinases by Phos-Tag SDS-PAGE. Journal of Proteomics. 255, 104485. DOI: https://doi.org/10.1016/j.jprot.2022.104485

[33] Jumrah, E., Sudding, Luqman, A.A., et al., 2024. Utilization of SDS-PAGE (Sodium Dodecyl Sulfate-Polyacrylamide Gel) Electrophoresis in Protein Purification. Hayyan Journal. 1(3), 7–12.

[34] Kumar, V., Kumar, N., Ghosh, U., et al., 2024. Predicting the Electrophoretic Mobility of Charged Particles in an Aqueous Medium. Langmuir. 40(31), 16521–16529. DOI: https://doi.org/10.1021/acs.langmuir.4c01939

[35] Tian, J., Barrat, J.-L., Kob, W., 2025. Influence of Preparation and Architecture on the Elastic Modulus of Polymer Networks. arXiv preprint. arXiv:2506.09670. DOI: https://doi.org/10.48550/arXiv.2506.09670

[36] Sakumichi, N., Yoshikawa, Y., Sakai, T., 2021. Linear Elasticity of Polymer Gels in Terms of Negative Energy Elasticity. Polymer Journal. 53(12), 1293–1303. DOI: https://doi.org/10.1038/s41428-021-00529-4

[37] Liu, X., Wu, J., Qiao, K., et al., 2022. Topoarchitected Polymer Networks Expand the Space of Material Properties. Nature Communications. 13(1), 1622. DOI: https://doi.org/10.1038/s41467-022-29245-0

[38] Hu, L., Han, Y., Rong, C., et al., 2022. Interfacial Engineering With Rigid Nanoplatelets in Immiscible Polymer Blends: Interface Strengthening and Interfacial Curvature Controlling. ACS Applied Materials

& Interfaces. 14(8), 11016–11027. DOI: https://doi.org/10.1021/acsami.1c24817

[39] Keledi, G., Hári, J., Pukánszky, B., 2012. Polymer Nanocomposites: Structure, Interaction, and Functionality. Nanoscale. 4(6), 1919–1938. DOI: https://doi.org/10.1039/C2NR11442A

[40] Yoon, S.J., Lee, S.J., Jeon, I.-Y., 2024. High-Performance Graphitic Nanoplatelets & High-Density Polyethylene Nanocomposites. Journal of Applied Polymer Science. 141(36), e55914. DOI: https://doi.org/10.1002/app.55914

[41] Suriano, R., Griffini, G., Chiari, M., et al., 2014. Rheological and Mechanical Behavior of Polyacrylamide Hydrogels Chemically Crosslinked With Allyl Agarose for Two-Dimensional Gel Electrophoresis. Journal of the Mechanical Behavior of Biomedical Materials. 30, 339–346. DOI: https://doi.org/10.1016/j.jmbbm.2013.12.006

[42] Lerman, L.S., Frisch, H.L., 1982. Why Does the Electrophoretic Mobility of DNA in Gels Vary with the Length of the Molecule? Biopolymers. 21(5), 995–997. DOI: https://doi.org/10.1002/bip.360210511

[43] Lumpkin, O.J., Zimm, B.H., 1982. Mobility of DNA in Gel Electrophoresis. Biopolymers. 21(11), 2315–2316. DOI: https://doi.org/10.1002/bip.360211116

[44] Rahmannezhad, J., Lee, H.S., 2024. Reptation Theory-Similar Deep Learning Model for Polymer Characterization from Rheological Measurement. Korea-Australia Rheology Journal. 36, 145–153. Available from: https://link.springer.com/article/10.1007/s13367-024-00091-4

[45] Mishra, G., Bigman, L.S., Levy, Y., 2020. ssDNA Diffuses Along Replication Protein A via a Reptation Mechanism. Nucleic Acids Research. 48(4), 1701–1711. Available from: https://academic.oup.com/nar/article/48/4/1701/5699673

[46] Thompson, J.W., Stretz, H.A., Arce, P.E., 2010. Preliminary Observations of the Role of Material Morphology on Protein-Electrophoretic Transport in Gold Nanocomposite Hydrogels. Industrial & Engineering Chemistry Research. 49(23), 12104–12110. DOI: https://doi.org/10.1021/ie100291b

[47] Asakura, S., Oosawa, F., 1954. On Interaction between Two Bodies Immersed in a Solution of Macromolecules. The Journal of Chemical Physics. 22(7), 1255–1256. DOI: https://doi.org/10.1063/1.1740347

[48] Bokobza, L., 2023. Elastomer Nanocomposites: Effect of Filler–Matrix and Filler–Filler Interactions. Polymers. 15(13), 2900. DOI: https://doi.org/10.3390/polym15132900

[49] Baek, K., Park, H., Shin, H., et al., 2021. Multiscale Modeling to Evaluate Combined Effect of Covalent Grafting and Clustering of Silica Nanoparticles on Mechanical Behaviors of Polyimide Matrix Composites. Composites Science and Technology. 206, 108673. DOI: https://doi.org/10.1016/j.compscitech.2021.108673

[50] Karim, M.R., Harun-Ur-Rashid, M., Imran, A.B., 2023. Effect of Sizes of Vinyl Modified Narrow-Dispersed Silica Cross-Linker on the Mechanical Properties of Acrylamide Based Hydrogel. Scientific Reports. 13(1), 5089. DOI: https://doi.org/10.1038/s41598-023-32185-4